

Digital Predistorted Inverse Class-F GaN PA with Novel PAPR Reduction Technique

Jingqi Wang, *Student Member, IEEE*, Yingjie Xu, and Xiaowei Zhu, *Member, IEEE*

State Key Lab of Millimeter Waves, Southeast University, Nanjing, Jiangsu, 210096, China
Email:jqwang@emfield.org

Abstract — In this paper, a digital predistorted inverse class-F GaN power amplifier with novel PAPR reduction technique, in which not only peaks but also valleys of signal are clipped to reduce the PAPR as much as possible, is presented. The inverse class-F PA is implemented by using Cree’s CGH40010 GaN HEMT with a 10W output power. Measurement results show that ACPR of the proposed PA decreases from -35.4dBc to -51.9dBc for a wideband OFDM signal with 20MHz bandwidth and 8dB PAPR after PAPR reduction. Drain efficiency of the PA is 31.3% at an average output power of 33.6dBm.

Index Terms —OFDM, peak-to-average power ratio, digital predistortion, power amplifier, inverse class-F, GaN

I. INTRODUCTION

Orthogonal frequency-division multiplexing (OFDM) allows efficient use of available spectrum due to the orthogonality feature of its subcarriers [1]. However a major drawback of OFDM is its high peak to average power ratio (PAPR) which causes a serious challenge for power amplifier design to meet both linearity and efficiency performances.

In order to achieve high efficiency, switching mode PAs, such as class-E, class-F, and inverse class-F [2-5] have been developed. However, these power amplifiers achieve high efficiency at the expense of poor linearity caused by the operation in saturation. Therefore, digital predistortion (DPD) technique is required to eliminate serious distortion of these power amplifiers.

For a digital predistorted power amplifier, the highest power efficiency is achieved at an operating output power back-off (OPBO) equals to the signal’s PAPR. Therefore, by reducing the signal’s PAPR, the power amplifier can operate at a lower operating OPBO and consequently the power efficiency is improved. Several PAPR reduction techniques have been reported [6]. PAPR reduction technique as a complementary technique to digital predistortion can also improve linearity of power amplifiers. The combination of PAPR reduction and digital predistortion leads to optimized performance in terms of linearity and efficiency [7]-[11].

This paper presents an inverse class-F power amplifier with high efficiency and linearity. The design methodology focuses on achieving the highest possible linearity performance while meeting the efficiency. The inverse class-F GaN PA is implemented by using Cree’s CGH40010 GaN HEMT with a 10W output power. The digital predistortion (DPD) is implemented with Hammerstein model. In order to address the

PAPR problem, a novel PAPR reduction technique which clips valley of signal in addition to peaks of signal is employed. The valley clipping removes low value of the envelope levels and is achieved by adjusting both the phase and magnitude of the signal using a circle-tangent shift approach [13]. Furthermore, to remove out-of-band distortion and minimize in-band distortion caused by PAPR reduction, an unused tone technique is used to restore the carrier data to the original values and leave optimized small residue values on the unused tones. Measurement results show that PAPR of a 20MHz bandwidth OFDM signal is reduced from 9.6dB to 8 dB. The adjacent channel power ratio (ACPR) decreased from -35.4dBc to -51.9dBc and the drain efficiency of the PA is 31.3% at 33.6dBm average output power. This proposed power amplifier achieves very high linearity and efficiency.

II. INVERSE CLASS-F POWER AMPLIFIER DESIGN

A. Circuit Topology

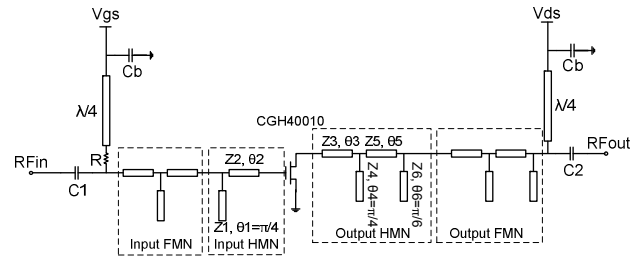


Fig. 1. Topology of inverse class-F power amplifier.

Ideally, an infinite number of even-harmonic resonators results in an inverse class-F mode with a half-sinusoidal voltage waveform and a square current waveform at the device output terminal. However, it is impractical to tune infinite number of harmonics in the microstrip design. In this paper, only the second and third harmonic load impedances are considered. Fig.1 shows the circuit topology of the inverse class-F PA with center frequency of 2.55GHz. The power transistor is Cree’s CGH40010 GaN HEMT. In order to satisfy the inverse class-F operation, the output harmonic matching network (HMN) provides proper second and third harmonic load impedances at the drain port of the transistor. By setting $\theta_4 = \pi/4$ (to control the 2nd harmonic) and $\theta_6 = \pi/6$ (to control the 3rd harmonic), the fundamental matching network (FMN)

will not affect the values of the harmonic impedances. On the input end, the input HMN provides proper second harmonic source impedance at the gate to improve the efficiency. All the harmonic impedances mentioned above are obtained by the harmonics load/source pull simulation tool in Agilent's Advanced Design System (ADS).

B. Implementation and Measurement

The inverse class-F PA is fabricated on the substrate Taconic RF-35 with dielectric constant of 3.5 and thickness of 30mil.

By setting $V_{gs}=3.6\text{GHz}$ and $V_{ds}=28\text{V}$, Fig.2 shows the measured drain efficiency (DE), power-added efficiency (PAE), output power and power gain for a 26dBm input power with the frequency swept from 2.5-2.6GHz. According to the figure, DE is greater than 52%, PAE is greater than 47.7% and output power is greater than 36.9dBm within the 100MHz bandwidth. The peak DE of 75.2% and peak PAE of 73% are observed at 2.55GHz with maximum output power and power gain of 41.4dBm and 15.4dB, respectively.

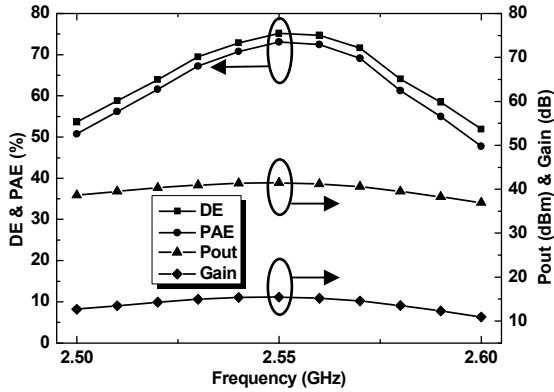


Fig. 2. Measured results vs. frequency with $V_{gs}=3.6\text{V}$, $V_{ds}=28\text{V}$ and $P_{in}=26\text{dBm}$.

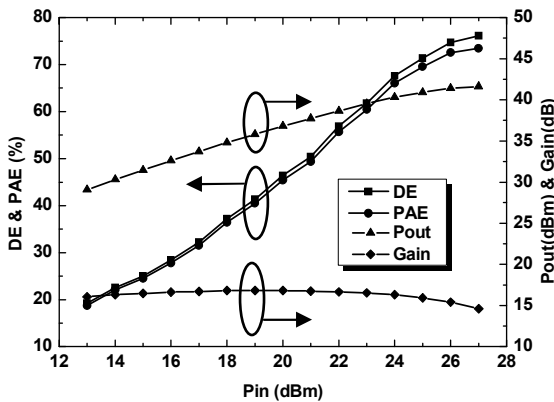


Fig. 3. Measured results vs. input power with $V_{gs}=3.6\text{V}$, $V_{ds}=28\text{V}$ and $f=2.55\text{GHz}$.

Driven by a 2.55GHz CW input signal with the power swept from 13dBm to 27dBm, the measurement results of the

inverse class-F PA are plotted in Fig.3. When the driven power comes to 27dBm, the DE and PAE are 76% and 73.5%, respectively. However, the power gain has been suppressed to 14.6dB, a 2.2dB suppression compared with the maximum power gain observed at 20dBm driven power.

III. PEAK-TO-AVERAGE POWER RATIO REDUCTION

PAPR of OFDM is the ratio between the maximum instantaneous power and the average power, defined by

$$PAPR = \frac{P_{peak}}{P_{average}} = \frac{\max \left[|x_n|^2 \right]}{E \left[|x_n|^2 \right]} \quad (1)$$

where x_n denotes an OFDM signal after IFFT, and $E[\cdot]$ denotes the expectation operator.

In order to decrease PAPR, most PAPR reduction approaches rely mainly on peak clipping, which makes P_{peak} , numerator of equation (1), smaller and thereby the PAPR is reduced. Obviously, increasing the denominator of equation (1) can also reduce the PAPR, that is to say, raising the expectation value of signal leads to PAPR reduction. Therefore, in our approach, not merely peaks are clipped, but also valleys of signal are considered as a way to reduce the PAPR.

One straightforward solution to clip the valleys of signal is to create a hole into the constellation diagram of the vector I/Q waveform, so that the magnitude of the envelope does not drop close to a zero value, namely "vector hole punching" [12].

A novel vector hole punching technique which removes low value envelope levels by adjusting both the phase and magnitude of the signal using a circle-tangent shift approach is presented. Some signal samples are plot in the constellation diagram, as shown in Fig.4, where the circle represents the valley clipping threshold and points A and B represent the signal samples. The trajectory travelling from A to B passes within an area that is close to the origin, which leads to a signal exceeds the threshold. To keep the signal away from zero, B is moved to B' and so that the B-B' trajectory line tangential to the circle, then the trajectory from A to B' will no longer pass inside the circle, that is to say, the valley will no longer exist.

In order to reduce the PAPR as much as possible, this valley clipping is combined with a Gaussian pulse based tone reservation technique. And furthermore, to remove out-of-band distortion and minimize in-band distortion caused by PAPR reduction, an unused tone technique is employed to restore the carrier data to original values after the hole punching and leave optimized small residue values on the unused tones. After the proposed PAPR reduction, OFDM signals which are close to the origin or exceed the peak clipping threshold are eliminated, and the vector of OFDM

signal is restricted within the range defined by valley clipping threshold and peak clipping threshold, as shown in Fig. 5.

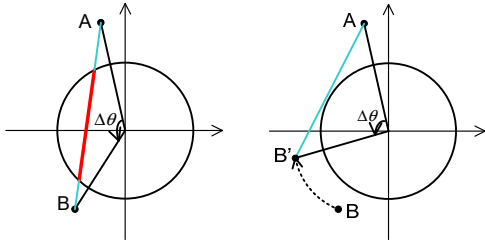


Fig. 4. Change phase to clip valley (Left: before the hole punching; Right: after the hole punching).

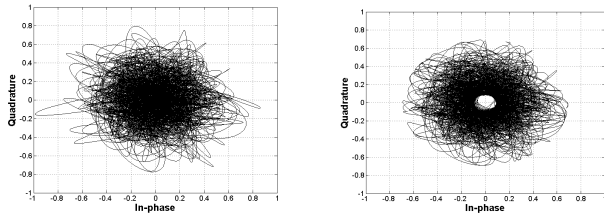


Fig. 5. Vector diagram of the OFDM signal (Left: before the PAPR reduction; Right: after the PAPR reduction).

IV. MEASUREMENT RESULTS

To valid the linearity and efficiency improvement of the proposed inverse class-F GaN power amplifier, a 2.55GHz 16QAM modulated broadband OFDM signal with 20MHz bandwidth and 9.6dB PAPR at 0.01% level of the complementary cumulative distribution function (CCDF) was employed.

The experimental validation system consists of a vector signal generator (Rohde & Schwarz SMBV100A), a vector signal analyzer (Agilent VSA-E4445A), a PC with Matlab and Agilent's 89600, the proposed inverse class-F GaN PA. The SMBV100A, E4445A and PC are connected via local area network (LAN). The configuration of the system is shown as Fig.6. PAPR reduction and digital predistortion is implemented in PC and the processed OFDM is transferred to the vector signal generator by LAN and then fed into the inverse class-F power amplifier.

The FFT size of the OFDM signal is 2048 and is over-sampled by a factor of 4. In this signal, there are 1669 data carriers and 381 unused tones, in which we chose 130 tones for the PAPR reduction and unused tone technique.

To suppress the signal distortion caused by PAPR reduction, we have chosen some appropriate, not excessive, PAPR thresholds. The valley clipping threshold equals 17% of the maximum magnitude of the signal, the peak clipping threshold equals 85%, and the magnitude threshold for circle-tangent shift m_t was 1% of the maximum magnitude value and the

phase threshold p_t was one degree. In this test, 10 iterations were conducted.

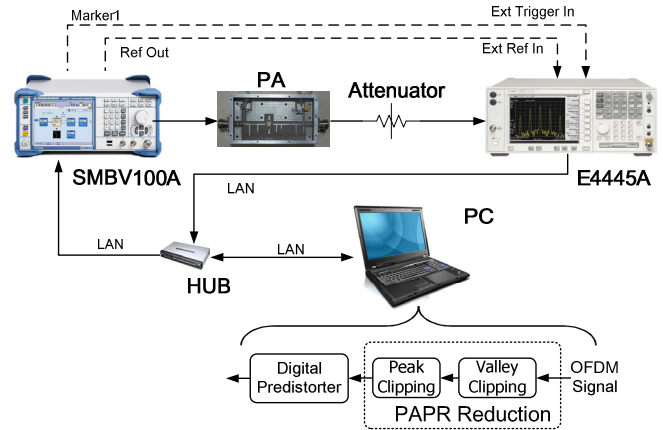


Fig. 6. Configuration of the validation system.

As shown in the complementary cumulative distribution function (CCDF) plot in Fig.7, the PAPR was reduced from 9.6dB to 8dB after the proposed PAPR reduction process, while the PAPR reduction is about 0.6dB after tone reservation process, which only clips peaks of the original signal. The proposed new PAPR reduction technique achieves lower PAPR by clipping both valley and peak signal.

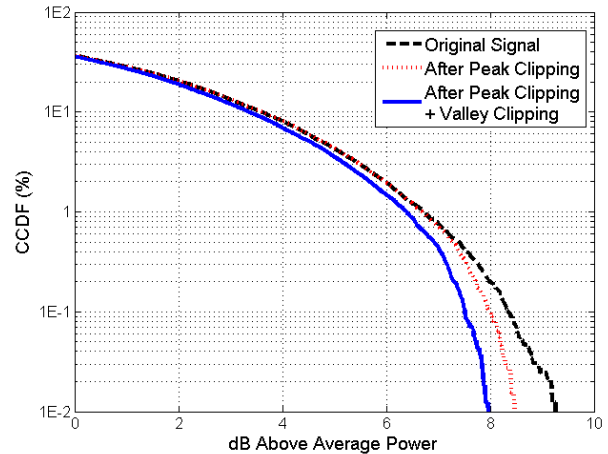


Fig. 7. CCDF plot of the OFDM signal.

Using the Hammerstein architecture, the inverse PA model (digital predistorter) can be established with the input and output I/Q samples of the PA. Since the PAPR of the clipped OFDM signal is 8dB and the saturated power of the PA is 41.6dBm, the PA is then forced to operate at 41.6-8=33.6dBm, a suitable back-off average output power, to compromise the efficiency and linearity. The drain efficiency of the PA is 31.3% at 33.6dBm average output power.

The baseband I/Q signals are modulated and up-converted to RF signal in SMBV100A, and then the RF signal is amplified and distorted by the PA. After attenuation, the RF output signal of PA is down-converted and demodulated by E4445A. Finally, the output I/Q samples are collected in VSA 89600 for modeling. In this experiment, the Hammerstein model achieves a normalized mean square error (NMSE) performance gets to below -40.5dB, which indicates great modeling accuracy. With the digital predistorter, the distortion of the PA can be fully compensated.

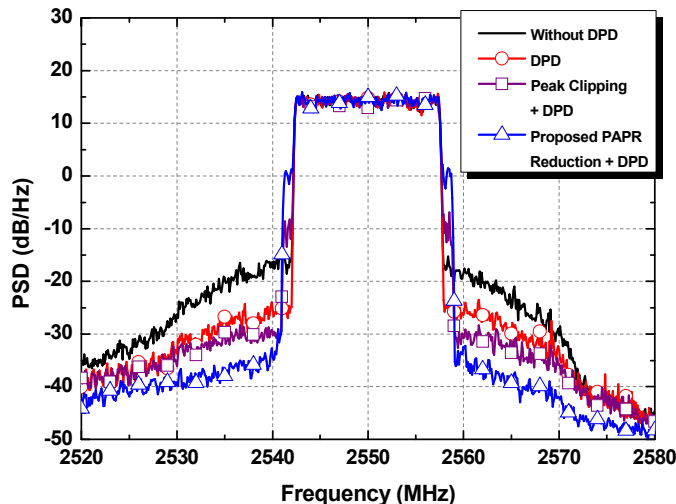


Fig. 8. Measured PSD of power amplifier output.

Fig.8 shows the measured PSD of the PA driven by 20MHz bandwidth OFDM signal. The black trace indicates the original output of the PA. The adjacent channel power ratio (ACPR) is -35.6dBc (lower) and -38dBc (upper) at an average output power of 33.6dBm. After DPD with Hammerstein, the output PSD of the PA is shown by the red trace, the ACPR of which is suppressed to -44.2dBc (lower) and -43.7dBc (upper). A slightly linearity improvement is achieved at this power level of the inverse class-F PA. When the baseband I/Q signal is processed by peak clipping, distorted by the digital predistorter, and then downloaded to SMBV100A as the input signal of the PA, the output PSD of the PA is shown by the purple trace, the ACPR of which equals to -46.6dBc (lower) and -48.2dBc (upper). Finally, after inserting valley clipping before peak clipping, the output ACPR of the PA comes to the lowest, which equals to -51.9dBc (lower) and -54.1dBc (upper).

V. CONCLUSION

In this paper, a linear inverse class-F GaN power amplifier with novel PAPR reduction and DPD technique is presented. The inverse class-F PA is implemented by using Cree's CGH40010 GaN HEMT with a 10W output power. And the PAPR reduction is proposed in which not only peaks, but also valleys of signal are clipped to reduced the PAPR as much as

possible. Measurement results show that the proposed inverse class-F GaN power amplifier achieve high linearity and power efficiency.

ACKNOWLEDGEMENT

This work was supported in part by National Key Technologies R&D Program of China under Grant 2010ZX03007-003-02 and in part by NSFC under Grant 60921063.

REFERENCES

- [1] R. Van Nee and R. Prasad. *OFDM for Wireless Multimedia Communications*. Artech House, 2000.
- [2] K. C. Tsai, and P.R. Gray, "A 1.9-GHz, 1-W CMOS class-E power amplifier for wireless communications", *IEEE Journal of Solid-State Circuits*, vol.34, no.7, pp. 962 – 970, 1999.
- [3] Y. S. Lee, and Y. H. Jeong, "A High-Efficiency Class-E GaN HEMT Power Amplifier for WCDMA Applications", *IEEE Microwave and Wireless Components Letters*, vol. 17, no.8, pp. 622 – 624, 2007.
- [4] D. Schmelzer, "A GaN HEMT Class F Amplifier at 2 GHz With >80% PAE", *IEEE Journal of Solid-State Circuits*, vol. 42, no. 10, pp. 2130 - 2136, October 2007.
- [5] A. Grebennikov, "High-efficiency transmission-line GaN HEMT inverse class F power amplifier for active antenna arrays," *Asia Pacific Microwave Conference*, pp. 317-320, December 2009.
- [6] S. H. Han, and J. H. Lee, "An overview of peak-to-average power ratio reduction techniques for multicarrier transmission", *IEEE Wireless Communications*, vol.12, no.2, pp. 56 – 65, 2005.
- [7] O. Hammi, S. Carichner, B. Vassilakis, and F. M. Ghannouchi, "Synergetic crest factor reduction and baseband digital predistortion for adaptive 3G Doherty power amplifier linearizer design," *IEEE Trans. Microw. Theory Tech.*, vol. 56, no. 11, part: 2, pp. 2602-2608, Nov. 2008.
- [8] R. Sperlrich, Y. Park, G. Copeland, and J. S. Kenney, "Power amplifier linearization with digital pre-distortion and crest factor reduction," *IEEE MTT-S International Microwave Symposium Digest, Fort Worth, TX*, vol. 2, pp. 669-672. Jun. 2004.
- [10] O.Hammi, S. Carichner, B. Vassilakis, and F.M. Ghannouchi, "Effects of crest factor reduction on the predistortion performance for multi-carrier 3G RF power amplifiers", *IEEE Microwave Symposium Digest*, pp. 1085 - 1088, 2009.
- [11] H. G. Ryu, T. P. Hoa, K. M. Lee, S. W. Kim, and J.S. Park, "Improvement of power efficiency of HPA by the PAPR reduction and predistortion", *IEEE Transactions on Consumer Electronics*, vol. 50, no. 1, pp. 119 – 124, 2004.
- [12] D. Rudolph, "Out-of-band emissions of digital transmissions using Kahn EER technique," *IEEE Trans. Microw. Theory Tech.*, 2002, 50:1979-1983.
- [13] J. Wang, A. Zhu, X. Zhu, and T. J. Brazil, "Vector Hole Punching Technique for OFDM Signals Using Circle-Tangent Shift and Unused Tones," *IEEE Trans. Microw. Theory Tech.*, pp. 2682-2691, 2009.